Published OnlineFirst September 5, 2019; DOI: 10.1158/0008-5472.CAN-19-0187

Translational Science

Cancer Research

Predictive Signatures Inform the Effective Repurposing of Decitabine to Treat KRAS–Dependent Pancreatic Ductal Adenocarcinoma

Carla Mottini[1], Hideo Tomihara[2], Diego Carrella[3], Alessia Lamolinara[4], Manuela Iezzi[4], Justin K. Huang[5], Carla A. Amoreo[6], Simonetta Buglioni[6], Isabella Manni[7], Frederick S. Robinson[5], Rosalba Minelli[5], Ya'an Kang[8], Jason B. Fleming[9], Michael P. Kim[8], Christopher A. Bristow[5], Daniela Trisciuoglio[10,11], Antonella Iuliano[3], Donatella Del Bufalo[10], Diego Di Bernardo[3], Davide Melisi[12], Giulio F. Draetta[2,5], Gennaro Ciliberto[13], Alessandro Carugo[5], and Luca Cardone[1]

Abstract

Mutated KRAS protein is a pivotal tumor driver in pancreatic cancer. However, despite comprehensive efforts, effective therapeutics that can target oncogenic KRAS are still under investigation or awaiting clinical approval. Using a specific KRAS–dependent gene signature, we implemented a computer-assisted inspection of a drug–gene network to *in silico* repurpose drugs that work like inhibitors of oncogenic KRAS. We identified and validated decitabine, an FDA-approved drug, as a potent inhibitor of growth in pancreatic cancer cells and patient-derived xenograft models that showed KRAS dependency. Mechanistically, decitabine efficacy was linked to KRAS–driven dependency on nucleotide metabolism and its ability to specifically impair pyrimidine biosynthesis in KRAS–dependent tumors cells. These findings also showed that gene signatures related to KRAS dependency might be prospectively used to inform on decitabine sensitivity in a selected subset of patients with KRAS–mutated pancreatic cancer. Overall, the repurposing of decitabine emerged as an intriguing option for treating pancreatic tumors that are addicted to mutant KRAS, thus offering opportunities for improving the arsenal of therapeutics for this extremely deadly disease.

Significance: Decitabine is a promising drug for cancer cells dependent on RAS signaling.

Introduction

Pancreatic ductal adenocarcinoma (PDAC) is one of the deadliest epithelial tumors, with an overall 5-year survival rate of only 8% (1). Poor prognosis is due to the limited efficacy of the therapeutic options, which are related to the heterogeneity of genetic mutations, multiple activated pathways, and dense stromal environment (2), making it difficult to identify potentially effective drugs. *KRAS* mutation is the predominant genetic event for precursor pancreatic intraepithelial neoplasia (PanIN)—the early stage of pancreatic cancer—that occurs in approximately 95% of cases (3, 4). Additional genetic alterations in tumor suppressor genes, such as *CDKN2A*, *TP53*, and *SMAD4*, are required for tumor progression and PDAC development (5). RAS protein belongs to small guanosine triphosphate hydrolase (GTPase) enzymes that play an essential role in regulating a wide range of cellular processes, such as cellular growth, survival, and differentiation (6). The *RAS* gene family includes *KRAS, N-RAS*, and *H-RAS* genes, and the oncogenic mutation in residues G12, G13, and Q61, which are the most common lesions in human tumors (7). These mutations compromise GTPase activity, inducing constitutive RAS signaling that results in abnormal proliferation and tumor growth (8). In PDAC, specifically, the most frequent point mutation is located at codon G12 of *KRAS* and leads to the activation of molecular pathways supporting tumor initiation, development, and maintenance (4, 8–10).

[1]Department of Tumor Immunology and Immunotherapy, IRCCS Regina Elena National Cancer Institute, Rome, Italy. [2]Department of Genomic Medicine, The University of Texas MD Anderson Cancer Center, Houston, Texas. [3]Telethon Institute of Genetics and Medicine (TIGEM), Napoli, Italy. [4]Department of Medicine and Aging Science, Center for Advanced Studies and Technology (CAST), G. D'Annunzio University, Chieti-Pescara, Italy. [5]Department of Therapeutics Discovery, The University of Texas MD Anderson Cancer Center, Houston, Texas. [6]Department of Pathology, IRCCS Regina Elena National Cancer Institute, Rome, Italy. [7]Animal Facility (SAFU), IRCCS Regina Elena National Cancer Institute, Rome, Italy. [8]Department of Surgical Oncology, The University of Texas MD Anderson Cancer Center, Houston, Texas. [9]Department of Gastrointestinal Oncology, Moffitt Cancer Center, Tampa, Florida. [10]Preclinical Models and New Therapeutic Agents Unit, IRCCS Regina Elena National Cancer Institute, Rome, Italy. [11]Institute of Molecular Biology and Pathology, National Research Council, Rome, Italy. [12]Department of Medicine, University of Verona, Verona, Italy. [13]IRCCS Regina Elena National Cancer Institute, Rome, Italy.

Note: Supplementary data for this article are available at Cancer Research Online (http://cancerres.aacrjournals.org/).

Corresponding Authors: Luca Cardone, IRCCS Regina Elena National Cancer Institute, Via Elio Chianesi 53, Rome 00144, Italy. Phone: 390652662939; Fax: 390652665523; E-mail: luca.cardone@ifo.gov.it; and Alessandro Carugo, The University of Texas MD Anderson Cancer Center, 1901 East Road, Houston, TX 77054. Phone: 713-745-0862; E-mail: ACarugo@mdanderson.org

Cancer Res 2019;79:5612–25

doi: 10.1158/0008-5472.CAN-19-0187

Published OnlineFirst September 5, 2019; DOI: 10.1158/0008-5472.CAN-19-0187

Specific gene expression signatures can be associated with oncogenic mutations and deregulated signaling pathways in tumors (11, 12). Several studies demonstrated the potential of using gene expression profiles of cancer cells to analyze oncogenic pathways, and such gene profiles can reflect the deregulation of specific pathways in cancers (11, 13). Oncogenic KRAS–specific signatures have been derived from *in vivo* and *in vitro* cancer models to identify critical effectors of KRAS (14–16). Interestingly, other lines of evidence demonstrated that, based on specific transcriptional profiles, it is possible to identify a subset of PDACs that are highly dependent on oncogenic KRAS molecular pathways (17). These sets of evidence reinforce the important role played by KRAS in a subset of advanced pancreatic carcinoma, other than its well-established role as a driver for premalignant pancreatic tumor lesions. In both cases, a cellular KRAS addiction has been experimentally proven, indicating that the direct targeting of KRAS or KRAS–dependent (KRAS-dep) phenotypes by specific inhibitors might provide clinical benefits for preventing PanIN or treating selected PDACs. Recently, a phase I/II clinical trial (NCT03600883) with an allele-specific inhibitor for the G12C mutant variant started (18), yet KRAS G12C mutations have been observed in only 1% of patients with PDAC (19). Despite comprehensive efforts by means of conventional drug design and discovery screenings, effective therapeutic inhibitors targeting the much more prevalent KRAS mutations (G12D, G12V, and G12R) have yet to be identified and reach the clinical setting (20).

Drug repositioning (i.e., the use of old drugs for a novel therapeutic indication) is a cost-effective approach to rapidly offer new therapeutic opportunities in the clinic. The repositioning of FDA-approved drugs to target oncogenic pathways that still lack effective inhibitors, such as KRAS, would be a relevant pharmacologic approach to inhibit oncogene-dependent tumor growth. We previously implemented a computational approach to repurpose FDA-approved drugs as inhibitors of oncogenic PI3K-dependent signaling (21). This strategy is based on the inspection of a drug–gene signature network with a "reverse" oncogene-specific gene signature, aiming to identify drugs able to revert the oncogenic gene signature toward a wild-type expression profile, thus acting as a potential inhibitor of oncogenic pathways (22, 23). This demonstrated that an oncogenic signature might successfully support computer-assisted *in silico* repositioning of drugs against a pathway or target once it is able to induce a robust gene expression profile.

Decitabine (5-aza-2′-deoxycytidine [DEC]) is a drug currently approved for the treatment of myelodysplastic syndromes and acute myeloid leukemia (24, 25). Decitabine is an analogue of nucleotide cytidine, carrying a carbon replacement with nitrogen residue at position 5. Once incorporated into DNA, such modification impairs the transfer of a methyl residue by DNA methyltransferase activity, leading to a broad DNA demethylation and, consequently, derepression of transcriptionally silenced DNA loci (26, 27). Moreover, decitabine belongs to a family of nucleotide analogues, such as gemcitabine, which has a well-established anticancer effect and is currently used for treating patients with PDAC. In addition to its ability to inhibit DNA polymerase, gemcitabine is known for its ability to interfere with nucleotide metabolism and dNTPs pool homeostasis. Indeed, gemcitabine is able to inhibit both ribonucleotide reductase (28, 29) and thymidylate synthase (30, 31), which are key enzymes necessary to maintain dNTPs pool *de novo* biosynthesis and homeostasis. Notably, similar targets have also been demonstrated for decitabine (32), and, potentially, aza-deoxyuridine monophosphate (dUMP) formation might also account for additional decitabine selective cytotoxicity. Thus, the anticancer mechanism of action (MoA) for nucleotide analogues might also be attributed to their ability to modify nucleotide homeostasis, thus affecting DNA synthesis or DNA repair (33).

In this study, by taking advantage of a KRAS–specific gene signature derived from the HPDE cell line expressing the $KRAS^{G12V}$ oncogene, we identified decitabine as an inhibitor of KRAS-dep tumor growth. We showed that pancreatic cancer cell lines carrying a gene expression signature that predicts KRAS activation and dependency displayed high sensitivity to the treatment with decitabine, whereas KRAS–independent (KRAS-indep) cell lines were less or not responsive. A similar response was observed in patient-derived xenograft (PDX)–PDAC models with a gene signature that predicts KRAS dependency. Mechanistically, decitabine toxicity in KRAS-dep PDACs is linked to the ability of decitabine to act as a nucleotide analog and interfere with pyrimidine biosynthesis. This leads to a decrease of deoxycytidine monophosphate (dCMP) and deoxythymidine monophosphate (dTMP) levels, both of which are essential to pyrimidine homeostasis, and to dUMP accumulation. Our data provide the experimental support to repurpose decitabine for the treatment of selected KRAS-dep patients with PDAC based on a gene signature screening.

Materials and Methods

Cell lines

Human pancreatic ductal epithelia (HPDE) cell lines and *KRAS* isogenic derivatives were obtained from Dr. D. Melisi (Department of Medicine, University of Verona, Verona, Italy). CAPAN-1 and PA-TU-8902 were provided by Dr. Giuseppe Diaferia (European Institute of Oncology, Milan, Italy). KP4 and PA-TU-8988T were provided by the cell culture facility at The University of Texas MD Anderson Cancer Center (UTMDACC; Houston, Texas). HPAF-II cell lines were provided by Dr. Michele Milella (Regina Elena National Cancer Institute, Rome, Italy). Cell line identities were genetically validated according to relative cell bank procedures and were cultured for fewer than 6 weeks after resuscitation. Upon passage, 10 cells were discarded. HPDE cells were discarded upon passage six. All cells were routinely tested for *Mycoplasma* contamination with a MycoFluor Mycoplasma Detection Kit (Thermo Fisher Scientific). The HPDE cells were cultured in Keratinocyte-SFM (Gibco) supplemented with human recombinant EGF and bovine pituitary extract. PA-TU-8902 and PA-TU-8988T cell lines were maintained in DMEM high glucose containing L-glutamine and sodium pyruvate and supplemented with 10% FBS (Gibco). CAPAN-1 and HPAF-II cells were grown in RPMI supplemented with 20% FBS (Gibco; CAPAN-1) or with 10% FBS (Gibco; HPAF-II), plus 1% glutamine (Gibco). KP4 cells were maintained in Iscove's modified Dulbecco's medium (Gibco), supplemented with 20% FBS and 200 mmol/L glutamine. All culture growth media were supplemented with 10,000 U/mL penicillin–streptomycin (Gibco).

PATC53, PATC124, and PATC153 cells were isolated from early passage (F1) PDAC-PDXs, as described in the Patient-derived samples section of the Materials and Methods (see below), and were maintained in culture for a maximum of two passages before being switched to DMEM 10% FBS and enrolled in phenotypic

Published OnlineFirst September 5, 2019; DOI: 10.1158/0008-5472.CAN-19-0187

studies and molecular profiling. All cells were kept in a humidified incubator at 37°C in 5 % CO_2 atmosphere.

Xenograft tumor experiments

Seven-week-old NOD/scid gamma (NSG) mice, purchased from The Jackson Laboratory, were subcutaneously injected with $1{,}5 \times 10^6$ PA-TU-8902, CAPAN-1, PA-TU-8988T, and KP4 cells diluted in 200 µL of 1:1 Matrigel (BD Biosciences) and media mixture, and treatment was approximately started 10 days after cells implantation when tumors reached approximately 40 mm^3. Decitabine dissolved in saline was injected intraperitoneally in mice at 1 mg/kg body weight 4 times a week for the first week and 3 times a week for the following 3 weeks; control mice received saline with DMSO alone. The animal health status was monitored daily. Tumor volume was measured every 3 days with calipers; body weight was also monitored. Tumor volume (mm^3) was calculated using the following formula: $V\,(mm^3) = L\,(mm) \times W\,(mm)^2/2$, where W is tumor width and L is tumor length. Mice were sacrificed when tumors were ulcerating, according to approved guidelines of the institution's animal ethics committee. Tumors and lungs were harvested, weighted, and fixed in formalin for histologic and IHC analysis. The Ethics Committee for Animal Experimentation of the Institute approved animal care and experimental procedures.

Patient-derived samples

Patient-derived samples were obtained from consented patients who signed a written informed consent under an institutional review board–approved protocol, LAB07-0854, chaired by Jason Fleming (UTMDACC).

PDAC–PDXs and PDX-derived primary cell cohorts

PDAC–PDXs were generated as described (34). Early-passage PDXs (F1) from primary human PDAC were harvested in cold HBSS (Gibco), and tumor cells were isolated through mechanical and enzymatic dissociation. Briefly, tumors were minced in very small pieces with scissors under sterile conditions before being processed with a Human Tumor Dissociation Kit (Miltenyi Biotec). After digestion, single isolated cells were seeded at high confluency on collagen-IV–coated plates (Corning) in DMEM/F12 (Gibco) supplemented with 10% FBS (Gibco), 1% bovine serum albumin (Thermo Fisher Scientific), 0.5 µmol/L hydrocortisone (Sigma-Aldrich), 10 mmol/L HEPES (Invitrogen), 100 ng/mL cholera toxin (Sigma-Aldrich), 5 mL/L insulin–transferrin–selenium (BD Biosciences), 100 IU/mL penicillin (Gibco), and 100 µg/mL streptomycin (Gibco). To get rid of fibroblasts in the culture, we periodically performed brief trypsinization (0.25% Trypsin-EDTA, Gibco). The purity of the human culture derived from PDX was confirmed over time by flow cytometry through the evaluation of HLA–ABC and mouse H-2Kd histocompatibility complex antigens (Becton Dickinson). Isolated human cells were maintained in culture for a maximum of two passages before being switched to DMEM 10% FBS and enrolled in phenotypic studies and molecular profiling. Early-passage (≤P3) PDX-derived cultures were transplanted in NSG-recipient mice to recapitulate original PDX architectural and structural features (35).

In vivo treatments of PDX-derived cells were performed by subcutaneously injecting 3×10^6 cells in NSG mice according to a procedure described above (see section Xenograft tumor experiments in Materials and Methods). All animal studies and procedures were approved by the UTMDACC Institutional Animal Care and Use Committee.

Results

Computational-assisted drug repurposing identified decitabine as a potential inhibitor of oncogenic KRAS addiction and associated gene signature

To explore the computational-assisted identification of FDA-approved drugs able to inhibit oncogenic KRAS and, consequently, the growth of KRAS–addicted tumors, we applied a validated method based on the MANTRA 2.0 algorithm to inspect a drug–gene signature network with a "reverse" (REV) oncogenic-specific signature (21). To this purpose, we took advantage of previously validated KRAS–specific gene expression signatures generated in different isogenic, not-transformed HPDE cell lines carrying the overexpression of $KRAS^{G12V}$ oncogene (Materials and Methods). These signatures generated new network nodes. Notably, nodes generated by different $KRAS^{G12V}$-overexpressing models (Materials and Methods) were statistically close in the network, regardless of the genetic model used (Supplementary Fig. S1A), thus confirming that these oncogenic signatures were robustly driven by the KRAS oncogene. The inspection of the MANTRA 2.0 network with the $KRAS^{G12V}$-REV node identified decitabine (Supplementary Fig. S1B) as, among top-scoring hits, the drug capable of generating $KRAS^{G12V}$-REV signature, thus potentially acting like an inhibitor.

To experimentally validate the MANTRA results, we treated HPDE-$KRAS^{G12V}$ cells with decitabine and demonstrated that decitabine was able to affect KRAS target gene expression as predicted by the MANTRA algorithm (Supplementary Fig. S1C). Next, we inspected the differential sensitivity of cells to decitabine treatment by exploiting oncogene addiction of HPDE-$KRAS^{G12V}$ compared with HPDE-KRAS wild-type. Notably, HPDE-$KRAS^{G12V}$ showed a 100-fold higher sensitivity than parental control cells (Supplementary Fig. S1D). Moreover, decitabine treatment induced cellular senescence in HPDE-$KRAS^{G12V}$ cells but not in isogenic wild-type cells, as demonstrated by the increase of β-galactosidase (β-gal staining; Supplementary Fig. S1E). This observation was in line with previous data reporting that the inhibition of senescence by oncogenic KRAS in HPDE can be prevented by decitabine treatment in PanIN models (36, 37). These results demonstrated that decitabine was able to hamper KRAS-dep proliferation in cells carrying oncogenic KRAS.

Oncogenic KRAS dependency predicted response to decitabine in selected KRAS–mutated PDAC cell lines

Next, we investigated whether decitabine might also efficiently inhibit tumor growth in the context of PDACs carrying oncogenic KRAS mutations and, most importantly, carrying a molecular dependency or "addiction" to KRAS. To this aim, we took advantage of previously validated methods to score KRAS activation by transcriptional gene profiles in PDAC to select a panel of KRAS-dep or KRAS-indep PDAC cell lines, in which a KRAS dependency has been experimentally validated (S-score; ref. 17). We also applied a score for KRAS molecular activation based on gene signatures as defined by MEK inhibition (L-score; ref. 15). We compared the two gene signatures in a panel of PDAC cell lines ($n = 49$) from the Cancer Cell Line Encyclopedia (CCLE; ref. 38), and we demonstrated a high degree of correlation among them

Published OnlineFirst September 5, 2019; DOI: 10.1158/0008-5472.CAN-19-0187

(Spearman $r = 0.64$, Fig. 1A). Signature scores allowed us to identify PDAC cell lines (HPAF-II, CAPAN-1, and PA-TU-8902) that are highly dependent on KRAS (hereafter referred to as dep-PDACs) as well as PDAC cell lines (KP4 and PA-TU-8988T) that, while presenting *KRAS* genetic mutations in hotspot sites, do show low S- and L-scores and thus were likely not dependent on KRAS (hereafter referred to as indep-PDACs; Fig. 1A; Supplementary Table S1). Indeed, treatment with decitabine showed that dep-PDAC cell lines displayed much higher sensitivity against decitabine than indep-PDACs (average IC_{50} of dep-PDAC cells = 0.12 μmol/L; average IC_{50} of indep-PDAC cells = 23 μmol/L; Fig. 1B). The interrogation of the Cancer Therapeutics Response Portal (CTRP) further confirmed that the response to decitabine treatment was significantly correlated with the L-score gene signature for KRAS dependency in a panel of KRAS–mutated PDAC cell lines (Spearman $r = -0.6$; Supplementary Fig. S2A). Accordingly, decitabine inhibited colony-forming capacity of dep-PDACs but not of indep-PDAC cells (Supplementary Fig. S2B). We found that decitabine inhibited cell proliferation in dep-PDAC cells through the induction of an G_2/M phases block in the cell cycle (Fig. 1C; Supplementary Fig. S2C and S2D). In contrast, indep-PDACs did not show cell-cycle arrest (Fig. 1C; Supplementary Fig. S2D). Thus, we selected a pair of dep-PDAC cells (PA-TU-8902 and HPAF-II) and a pair of indep-PDAC cells (KP4 and PA-TU-8988T) to investigate the essential mechanism inducing cell growth arrest. Cell size (Fig. 1D; Supplementary Fig. S2E) as well as β-gal staining (Fig. 1E) showed a statistically significant increase in dep-PDACs upon decitabine treatment, indicating that decitabine was able to induce cellular senescence, similar to HPDE-$KRAS^{G12V}$–treated cells. Again, decitabine affected cell-cycle irreversibly because removal of decitabine did not result in rescuing cell proliferation (Supplementary Fig. S2F), thus confirming a senescence phenotype. In contrast, indep-PDACs did not show an increase in cell size, or induction of senescence (Fig. 1D and E; Supplementary Fig. S2E), confirming that the observed mechanisms were involved in the differential response to decitabine treatment. On the basis of cell-cycle results, we suspected that decitabine might induce DNA damage. Immunofluorescence analysis of decitabine-treated dep-PDAC demonstrated a strong induction of phospho-H2AX–positive foci, an early marker of DNA damage, compared with DMSO-treated cells (decitabine = 40% positive foci vs. DMSO = 5% positive foci) and compared with indep-PDACs (Fig. 1F; Supplementary Fig. S2G). However, dep- and indep-PDAC had similar responses to DNA damage-inducing agents (Supplementary Fig. S2H), thus ruling out the possibility that dep-PDACs had an intrinsic increased sensitivity for DNA damage compared with indep-PDACs. Altogether, these data indicated that decitabine was able to affect the viability and proliferation in selected PDAC cell lines presenting oncogenic KRAS dependency, as indicated by high KRAS gene signature scores, and that molecular signatures might be prospectively used to inform on KRAS dependency and predict sensitivity to decitabine.

Decitabine specifically inhibited growth of KRAS-dep PDAC-derived xenograft tumors

To validate the efficacy of decitabine treatment against selected pancreatic cancer *in vivo*, we implanted dep-PDAC or indep-PDAC cell lines subcutaneously. The dep-PDACs tumors in DMSO-treated mice grew significantly more than tumors in decitabine-treated mice (Fig. 2A and B; Supplementary Fig. S3A), demonstrating that decitabine had antitumor activity *in vivo* against dep-PDAC tumors. In contrast, the growth of decitabine- or DMSO-treated tumors did not show any significant differences in indep-PDAC tumors–derived xenografts (Fig. 2C and D; Supplementary Fig. S3A), indicating the lack of *in vivo* efficacy in agreement with *in vitro* results.

To investigate whether decitabine mediated DNA damage *in vivo*, IHC studies were performed. Consistently with *in vitro* experiments, decitabine treatment resulted in increased staining of phospho-H2AX nuclei in dep-PDAC tumors. In addition, decitabine-treated tumors showed a reduction in the percentage of Ki67-positive cells compared with DMSO-treated tumors (Fig. 2E). In contrast, IHC analysis of the same markers in indep-PDAC tumors treated with decitabine demonstrated no significant differences compared with DMSO counterparts (Fig. 2E).

Hematoxylin and eosin analysis of lung tissue sections derived from xenograft models demonstrated that tumors generated by both KRAS dep- and indep-PDAC cells were able to induce lung metastases (Fig. 2F; Supplementary Fig. S3B). Notably, decitabine treatment significantly reduces the number of lung metastases observed in xenograft models generated by KRAS dep-PDAC cells PA-TU-8902 and CAPAN-1 but not in the xenograft mice models generated by KRAS indep-PDAC cells (Fig. 2F; Supplementary Fig. S3B). All together, these data indicated that decitabine treatment *in vivo* was able to selectively inhibit tumor growth and metastatic diseases generated by KRAS-dep tumors.

Dep-PDACs depend on active KRAS–MEK pathway

Our results demonstrated that decitabine was more effective in KRAS–mutated PDAC models carrying molecular dependency on the KRAS pathway, as scored by specific gene signatures (Fig. 1A; Supplementary Fig. S2A). To further validate the KRAS dependency in dep-PDAC models, we tested the differential sensitivity of cellular models after treating cells with trametinib, which is a specific inhibitor of the MEK protein that is one of the downstream molecular targets activated by KRAS. Trametinib was strongly efficacious in inhibiting the proliferation of dep-PDAC cell lines (PA-TU-8902, CAPAN-1, and HPAF-II; average IC_{50}: = 0.03 μmol/L, $n = 4$; Fig. 3A), whereas indep-PDAC cells were more resistant (average IC_{50}: = 20 μmol/L; $n = 4$; Fig. 3A). Interestingly, the inhibition of cell proliferation in trametinib-treated cells was associated with cellular senescence in dep-PDAC, as scored by β-gal–positive cells (Fig. 3B and C), indicating that the KRAS/MEK axis was essential to promote resistance to senescence. However, trametinib treatment did not induce DNA damage (Fig. 3D and E), indicating that the underlining MoA was likely different compared with decitabine. These data confirmed that (i) dep-PDAC cellular models were effectively more dependent on the KRAS/MEK axis than indep-PDAC cells; and (ii) the inhibition of this specific KRAS-dep target, similar to decitabine, elicited a selective senescence in dep-PDAC models but not DNA damage.

Because trametinib and decitabine are both FDA-approved anticancer drugs and because they showed a different cellular effect on dep-PDAC cells, we investigated the potential effects of the combination of these drugs. The cytotoxicity of the trametinib-plus-decitabine combination was evaluated using the Combination Index (CI) method (39, 40). Supplementary Figure S4 shows plots of the CI for the interaction between the two drugs. Our data showed that, for all concentration tested ranging from

Published OnlineFirst September 5, 2019; DOI: 10.1158/0008-5472.CAN-19-0187

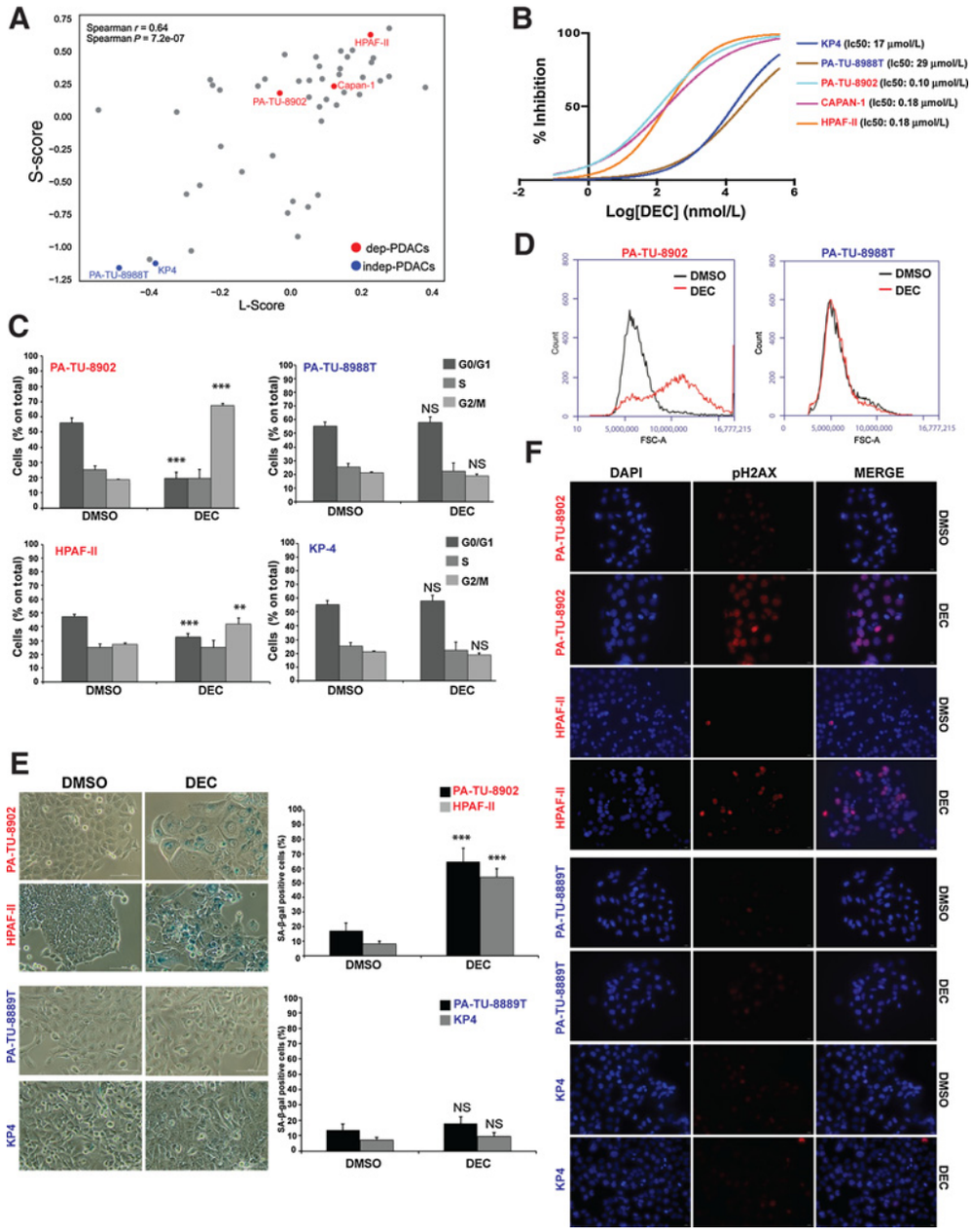

Figure 1.

A, Scatter plot comparing S-scores versus L-scores in 49 pancreatic cell lines calculated from the RNA sequencing data released by the CCLE Consortium. Selected cell lines with low or high S-/L-scores are indicated in blue or red, respectively. **B,** Determination of DEC′ inhibitory concentration (IC_{50}) in selected PDAC cell lines. The indicated cell lines were plated and grown for 6 days with different doses of decitabine, ranging from 0.001 µmol/L to 20 µmol/L. Cell viability was then assayed by the ATP-based CellTiter-Glo assay. Graphs report the percentage of inhibition compared with DMSO-treated cells ($n = 5$). IC_{50} calculation showed an intrinsic resistance of indep-PDAC cells. **C,** Decitabine induced a robust cell-cycle block at G_2/M phases of dep-PDACs but not of indep-PDACs. Cells were treated with high doses (1.25 µmol/L) of decitabine or DMSO for 3 days and then assayed by FACS analysis of propidium iodide-stained cells. Histograms show mean ± SD ($n = 4$). **D** and **E,** Decitabine-induced cellular senescence in dep-PDAC. **D,** Cellular size was quantified by FACS analysis. Representative plot of size analysis ($n = 3$) of dep-PDAC and indep-PDAC cells, treated for 5 days with DMSO (black line) or decitabine (red line). **E,** Left, representative images of β-gal staining after 5 days of treatment with DMSO or decitabine of indicated cells. Scale bar, 100 µmol/L). Right histograms, quantification of senescent cells by measuring senescence-associated β-gal–positive cells after 5 days of treatment with DMSO or decitabine. Histograms show mean ± SD. **F,** Decitabine-induced DNA damage in dep-PDACs. Representative images of immunofluorescence analysis of cells treated with DMSO or decitabine (1.25 µmol/L) and stained with anti-phospho-H2AX antibody, a molecular marker of DNA damage. For each experimental replicate ($n = 4$), cells were counted ($n = 100$), and the percentage of positive stained cells was reported. Scale bar, 10 µm. Quantification for these experiments is provided in Supplementary Fig. S2G. Statistical significance was calculated by two-tailed *t* test. **, $P \leq 0.01$; ***, $P \leq 0.001$; NS, not significant.

Published OnlineFirst September 5, 2019; DOI: 10.1158/0008-5472.CAN-19-0187

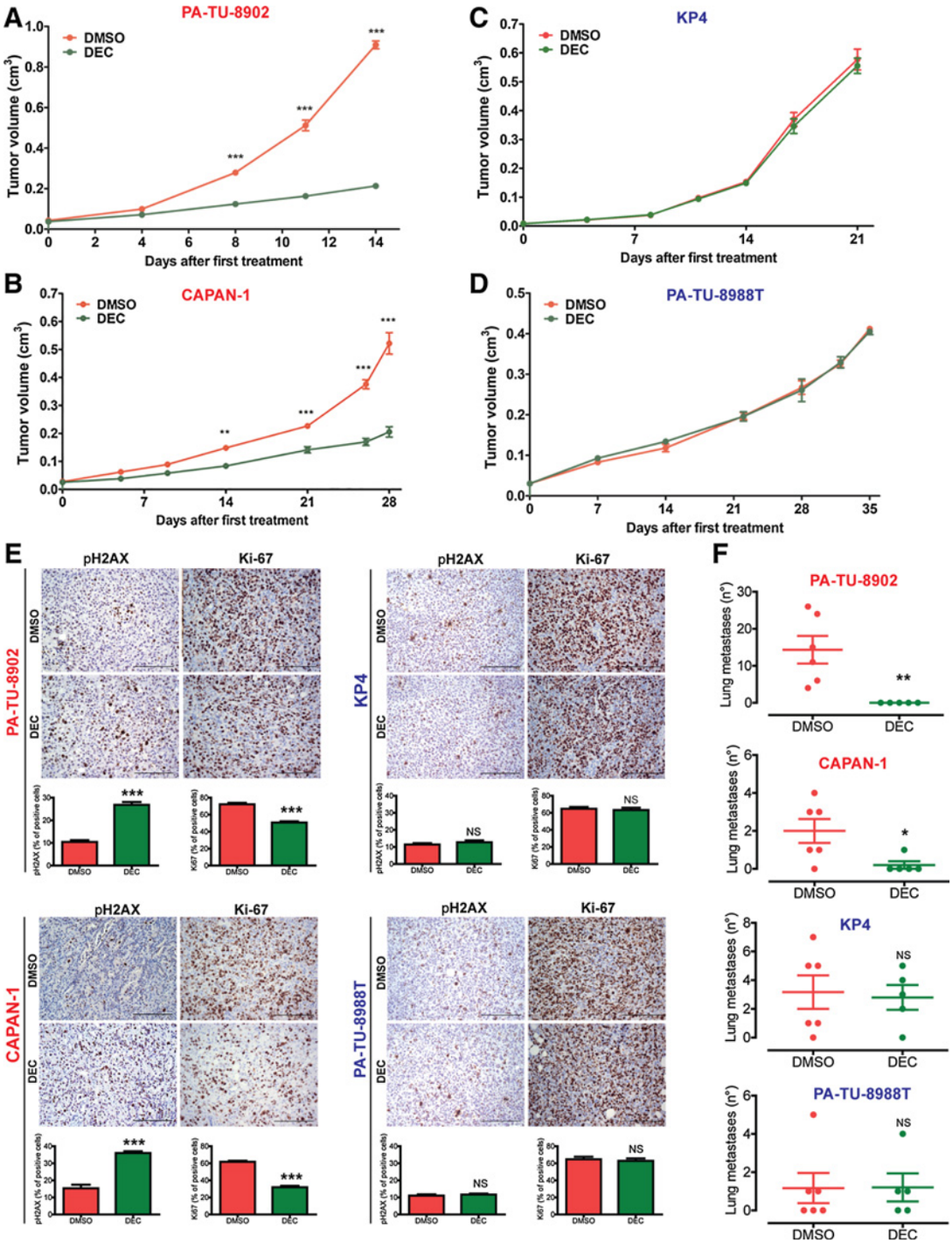

Figure 2.

Decitabine inhibited xenograft tumor growth and the development of lung metastases. **A–D,** Tumor growth kinetics of mice injected subcutaneously with PA-TU-8902, CAPAN-1, PA-TU-8988T, and KP4 cells and treated i.p. with DMSO (red line) or decitabine (green line). Data are mean ± SEM of volumes. Differences in tumor volume were evaluated using a two-way ANOVA test analysis. **, $P < 0.01$; ***, $P < 0.001$. NS, not significant. **E,** Representative images of IHC staining for phospho-H2AX and Ki67 of tumor sections from mice treated intraperitoneally with DMSO or decitabine until tumor resection. Scale bar, 100 μm. Magnification, ×200. Histograms show the quantification of the percentage of phospho-H2AX- and Ki67-positive cells. Statistical significance was calculated by two-tailed *t* test analysis. ***, $P < 0.0001$. **F,** Decitabine inhibited the development of lung metastases in xenograft tumor models of KRAS dep-PDAC cells. Histograms show the quantification of the number of lung metastases by hematoxylin and eosin staining of lung tissue sections from mice models shown in Fig. 2A–D. Differences in the number of metastases were evaluated using a Mann–Whitney test analysis. *, $P < 0.05$; **, $P < 0.001$.

Published OnlineFirst September 5, 2019; DOI: 10.1158/0008-5472.CAN-19-0187

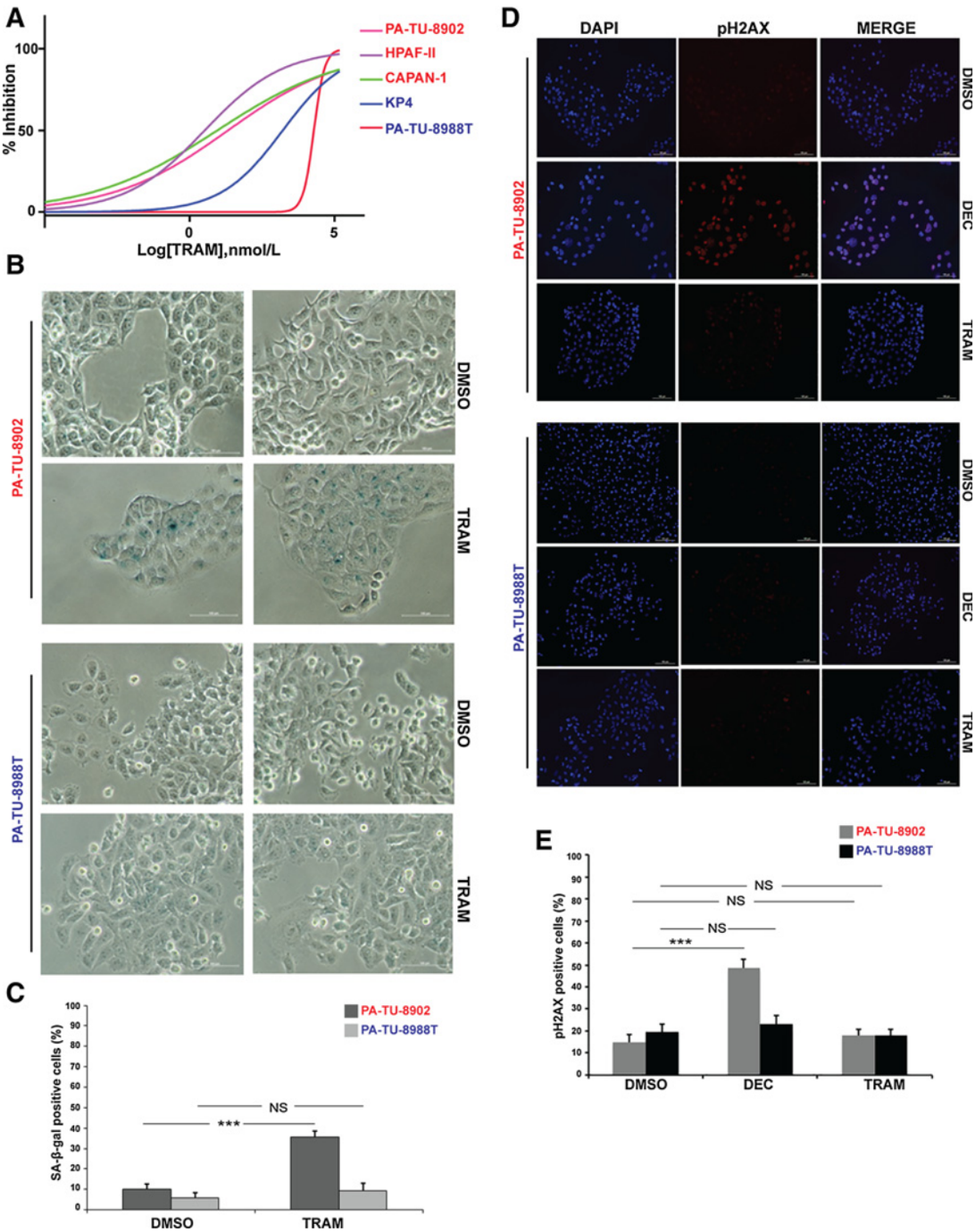

Figure 3.

A, The indicated dep-PDAC and indep-PDAC cells lines were treated with trametinib (TRAM) for 72 hours for the determination of IC_{50}. Different doses of trametinib, ranging from 0.001 μmol/L to 150 μmol/L, were used. Cell viability was then assayed by the ATP-based CellTiter-Glo assay. Graphs report the percentage of inhibition compared with DMSO-treated cells ($n = 4$). **B,** Trametinib-induced cellular senescence in dep-PDAC but not in indep-PDAC. Representative images of β-gal staining after 3 days of treatment with DMSO or trametinib of indicated cells. Scale bar, 100 μm. **C,** β-gal staining after 3 days of treatment with DMSO or trametinib of indicated cells was quantified. Histograms in this figure show mean ± SD. $n = 4$. **D,** Trametinib did not induce DNA damage. Representative images of immunofluorescence analysis for phospho-H2AX marker of PA-TU-8902 and PA-TU-8988T cells treated with trametinib or DMSO for 3 days. Cells were also treated with 1.25 μmol/L decitabine (DEC) as positive control. **E,** Quantification of immunofluorescence analysis described in **D**. For each experimental replicate ($n = 4$), cells were counted ($n = 100$), and the percentage of positive stained cells was reported (right). Histograms in this figure show mean ± SD. Statistical significance was calculated by two-tailed *t* test. ***, $P \leq 0.001$; NS, not significant.

Published OnlineFirst September 5, 2019; DOI: 10.1158/0008-5472.CAN-19-0187

0.25× to 4× of the IC_{50} concentrations, the drug combination had significant synergistic effects in both dep-PDAC cells tested (Supplementary Fig. S4, top). An r value of 0.95 or above indicated good conformity of the dose-effect data with respect to the median-effect principle. The r values for all the experiments were 0.99 or higher. In particular, when HPAF-II cells were treated at IC_{50} concentrations, this corresponded to a CI value of 0.67, indicating synergism. As the concentration of the trametinib and decitabine combination increased, the CI value decreased, indicating increased synergism (Supplementary Fig. S4, bottom left). At the IC_{95} concentration, the CI values were 0.25, indicating a strong synergism. Similarly, PA-TU-8902 cells treated with the calculated IC_{50} for both drugs demonstrated a CI value of 0.48, indicating a synergic combination (Supplementary Fig. S4, bottom right). As the concentration of trametinib and decitabine used in combination increased, the combined cytotoxic effects fell into slight synergism (CI = 0.95) at IC_{95}, which was much less effective than the treatments with lower doses. Overall, these results indicate the potential for synergic combinatorial treatment of trametinib and decitabine on dep-PDAC models across a large range of concentrations.

The vulnerability of dep-PDACs to decitabine is based on the impairment of *de novo* pyrimidine biosynthesis

Decitabine is an analogue of cytidine, largely used as a DNA demethylating agent (26). Next, we investigated whether the demethylation activity of decitabine was responsible for the target vulnerability of dep-PDAC compared with indep-PDAC. If this was the case, one could predict that the direct inhibition of DNA-methyltransferase (DNMT) activity, by means of specific DNMT inhibitors, would elicit a differential cytotoxic activity as well. Our results showed that, unexpectedly, both dep- and indep-PDACs cells had a similar response rate to either SG-1027 or RG-108 DNMT inhibitors (Fig. 4A and B). Moreover, cell viability and proliferation of both cellular models were relatively resistant to DNMT inhibition. These results argued against DNMTs as primary targets of decitabine in dep-PDACs.

Decitabine belongs to a family of nucleotide analogues, such as gemcitabine, with a well-established anticancer effect currently used for treating patients with PDAC. Interestingly, we observed that a low concentration of gemcitabine induced a strong and selective cell growth inhibition against dep-PDAC but not in indep-PDAC cells (Fig. 4C). This effect was linked to the induction of cellular senescence in dep-PDAC cells, thus mirroring decitabine effects (Fig. 4D). Moreover, the inspection of the CTRP showed a significant, even though not perfect, correlation for the sensitivity to decitabine and gemcitabine in a panel of PDAC cell lines (Spearman r = 0.54; Fig. 4E). Given the ability for both gemcitabine and decitabine to interfere with nucleotide metabolism and dNTPs pool homeostasis (31–33), and because the inhibition of pyrimidine biosynthetic enzymes showed a synthetic lethal vulnerability in mutant KRAS–driven cancers (10, 41, 42) we hypothesized that decitabine might affect dep-PDAC viability based on interfering with nucleotide metabolism. To directly address this hypothesis, we performed an untargeted LC/MS–based metabolomics analysis of polar metabolites isolated from both dep- and indep-PDAC cells upon treatment with decitabine. Our studies demonstrated that treating PDAC cells for 24 hours with decitabine induced a regulation of a number of different metabolites on dep- and indep-PDAC cells (Fig. 4F). Metabolite set enrichment analysis showed that, among the different analyzed pathways, pyrimidine metabolism ranked as the top significant listed pathway that was regulated selectively on dep-PDAC cells ($P < 0.05$; Fig. 4G), whereas no statistically significant pathway enrichment was observed on indep-PDAC (Supplementary Fig. S5). Notably, metabolites belonging to the phosphatidylethanolamine biosynthesis pathway, which is also implicated in the homeostasis of cytidine nucleotide, was also significantly affected by decitabine ($P < 0.05$; Fig. 4G). The analysis of enriched metabolites into the pyrimidine pathway (Fig. 4H) demonstrated that the treatment with decitabine increased specifically in dep-PDACs cells but not in indep-PDAC cells, the level of precursors of the pyrimidine *de novo* biosynthesis such as *N*-carbamoyl-L-aspartate ($log_2FC = 2.5$), dUMP ($log_2FC = 1.5$), deoxyuridine ($log_2FC = 0.66$), and uridine ($log_2FC = 0.5$). Concurrently, decitabine induced the downregulation of dTMP ($log_2FC = -0.86$) and dCMP ($log_2FC = -1.85$) levels, thus demonstrating the ability of decitabine to interfere with pyrimidine homeostasis and nucleotide pools specifically in KRAS-dep PDACs.

KRAS dependency inferred by molecular signatures predicts sensitivity to decitabine in selected KRAS–mutated PDX-PDAC models

To further investigate the efficacy of decitabine against selected PDAC populations, we took advantage of matched patient-derived primary cellular models and PDXs (34) that represent more reliable, patient-like experimental systems (43–45). First, we monitored whether transcriptional-informed KRAS dependency might be also associated with PDAC patient–derived primary cell models and whether the S-score and/or the L-score signature could assist in predicting molecular dependency and drug response in these more sophisticated experimental models. The initial profiling of a combined cohort of PDAC patient–derived primary cells and CCLE cells comprising 102 cases confirmed a good correlation level (Spearman $r = 0.61$) between the two classification methods (Fig. 5A), validating the relevance and reliability of these molecular signatures also in patient-derived scenarios.

To formally prove that KRAS dependency inferred by gene signature can be deployed to predict decitabine sensitivity in patient-derived models, we treated *in vitro* selected cases of KRAS-dep and -independent PDAC patient–derived cells (PATCs) as informed by gene signature (Fig. 5A). Our results confirmed a strong antiproliferative effect on dep-PDAC–PDX-derived cells (PATC124 and PATC53), resulting in estimated IC_{50} values lower than 1 μmol/L for decitabine (Fig. 5B). In contrast, a PDX–PDAC-derived model, with no KRAS dependency (PATC153), displayed resistance to decitabine treatment with an IC_{50} at least 10 times higher than the dep-PDAC models (Fig. 5B). Similar to our findings with CCLE cell lines, KRAS-dep PDX-derived PDAC models experienced cell-cycle arrest, senescence, and increase of phospho-H2AX–positive foci upon decitabine treatment (Fig. 5C–E; Supplementary Fig. S6A–S6D), further confirming the drug MoA in responder models. To validate that KRAS dependency inferred by gene signature can be deployed to predict sensitivity to decitabine *in vivo*, we transplanted and treated one dep- and one indep-PDAC patient–derived model. Once again, dep-PDAC tumors (PATX53) displayed significant growth inhibition upon decitabine treatment compared with DMSO-treated animals (Fig. 5F). In contrast, no significant differences in growth were detected between decitabine- or DMSO-treated tumors in

Published OnlineFirst September 5, 2019; DOI: 10.1158/0008-5472.CAN-19-0187

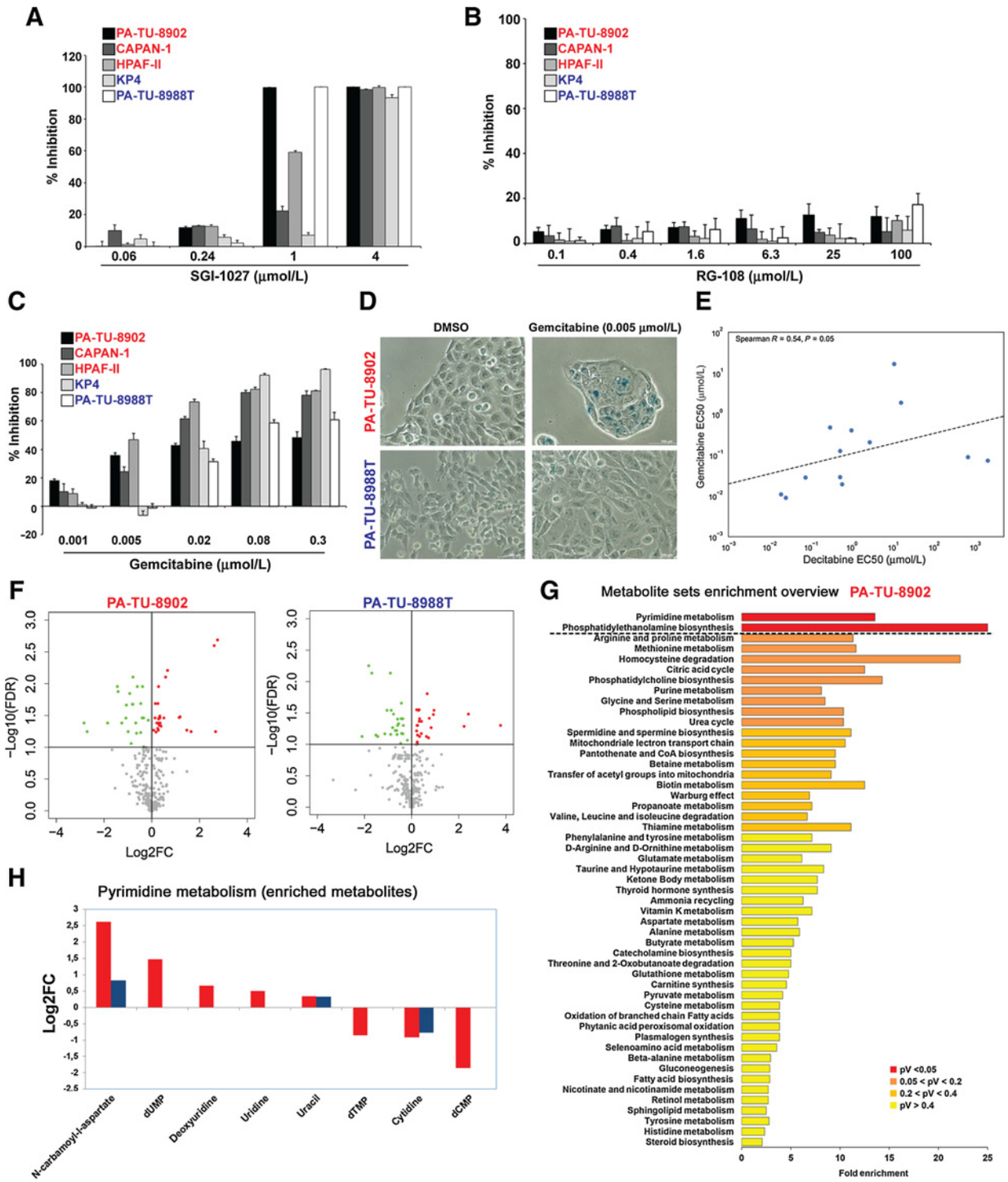

Figure 4.

A and **B,** DNA methyltransferase inhibitors did not differentially affect the proliferation of dep-PDAC or indep-PDAC cells. The indicated cell lines were treated for 6 days at the indicated doses of inhibitors. Cell viability was assayed by ATP-based assay. Graphs report the percentage of inhibition of cell viability, compared with DMSO-treated cells ($n = 4$). **C,** Dep-PDACs showed increased response to low doses of gemcitabine. Cells were treated with the indicated concentration of gemcitabine, and the percentage of inhibition of cell viability was reported ($n = 3$). **D,** Low dose of gemcitabine induced cellular senescence in dep-PDAC but not in indep-PDAC. Cells were treated with gemcitabine for 72 hours and then analyzed by β-gal staining ($n = 3$). **E,** Scatter plot comparing gemcitabine and decitabine EC_{50} (μmol/L) values in 13 pancreatic cell lines from the CTRP. **F,** Volcano plots of metabolites in PA-TU-8902 cells (left) and PA-TU-8988T cells (right) treated with 1.25 μmol/L decitabine for 24 hours. (*Continued on the following page.*)

Published OnlineFirst September 5, 2019; DOI: 10.1158/0008-5472.CAN-19-0187

indep-PDAC PATX153 xenograft experiments (Fig. 5G). IHC staining for Ki67 and phospho-H2AX proved decitabine MoA true also in a more patient-resembling context (Fig. 5H and I; Supplementary Fig. S6E and S6F). Overall, our data demonstrated that predicting decitabine sensitivity in PDAC patient–derived cells by a *KRAS* gene signature–based approach is feasible, similar to CCLE cells, and addiction does correlate with strength of the molecular signatures.

To further inform on the clinical translation of our findings, we classified a cohort of PDAC–PDXs developed at UTMDACC ($n = 49$) using the two KRAS-dep gene signatures (Fig. 5J; Supplementary Fig. S6G). In this case, we noted that the correlation among S-score and L-score is lower than what we previously detected for adherent cultures (Spearman $r = 0.23$), even though both signatures are able to properly segregate the matched PDX models for which we observed differential decitabine sensitivity in PDX-derived cells and transplants. Remarkably, we observed a similar correlation value (Spearman $r = 0.25$) between the two KRAS-dep gene signatures when we analyzed transcription profiles of patients with PDAC extrapolated from The Cancer Genome Atlas collection (Fig. 5K). Altogether, these findings support a classification strategy, based on the combined application of the two gene signatures, which could be prospectively used to inform on KRAS dependency and, potentially, predict sensitivity to decitabine in selected patients with KRAS–mutated pancreatic tumor.

Discussion

Despite the genetic and clinical relevance of the KRAS oncogene in multiple malignancies, the clinical demonstration of effective pharmacologic inhibition of KRAS and KRAS-dep cellular addiction for treating tumors is still pending. Aiming to meet this need, we applied an *in silico* drug discovery approach based on the computer-assisted inspection of a drug–gene network. For the first step, this process required handling an oncogene-driven genetic signature. The generation of a KRAS–specific signature from pancreatic models seemed to be appropriate considering (i) the high penetrance of KRAS mutations that are present in almost 98% of PDACs; and (ii) modeling this mutation in the context of HPDE cells, to derive a robust and specific KRAS–driven gene signature, is a physiologic approach recapitulating the KRAS biology and molecular effects, KRAS being a genetic mutation occurring very early during pancreatic cancer development and leading to precancerous lesions (PanIN). This method identified decitabine as a potential inhibitor of mutated KRAS-dep gene signature.

We validated the potential for using decitabine in a selected subset of patients with PDAC, whose dependency and activation of KRAS oncogene were scored by means of transcriptional signatures. Notably, we showed, for the first time, that such scores effectively identified dependency of KRAS in the context of PDAC patient–derived models, which is a more reliable, patient-like experimental system, thus opening the opportunity for selectively testing tailored compounds against KRAS into PDX models. Furthermore, our data refined the predictive capability of two previously reported KRAS-dep gene signatures identified in *in vitro* contexts, highlighting the importance of translational studies in reducing the risk of failure in clinical applications. Interestingly, our study unraveled an *in vivo* discrepancy between the two KRAS-dep gene scores that could reflect the different approaches used to derive such scores (15, 17) and potentially be associated with differences in how microenvironment can influence gene signatures, in particular the S-score. Indeed, classification of PDAC–PDXs using S-score better matched the molecular subtypes recently identified in patients with PDAC by applying tumor-specific factors (Supplementary Fig. S6H; refs. 43, 44). On the other hand, L-score might be associated with a higher degree of cell-autonomous signature, which is potentially less influenced by microenvironmental components and potentially less affected by *in vitro*/*in vivo* transition. These findings, even though based on a limited number of cases, further support the conclusion that a combined S-score/L-score molecular signature might be a robust predictive tool to infer oncogene dependency from tumor biopsy or PDX models for personalized patient therapies. In this regard, KRAS dependency, more than genetic mutations, seems actionable for a synthetic lethal approach with decitabine treatment. Because KRAS dependency by a molecular signature can be also identified in lung (17) and colon (46–48) tumors, it is worth investigating whether decitabine could be also effective for treating such malignancies in the context of KRAS dependency.

We showed that, in a subset of PDAC cells with dependency on the KRAS oncogene, decitabine had an intrinsic ability to induce cell-cycle arrest and DNA damage by a mechanism that is independent on its DNMT inhibitor activity. Indeed, specific DNMT inhibitors failed to be selectively toxic against dep-PDAC, and, accordingly, DNMT inhibition, *per se*, was not enough to induce cell-cycle arrest in dep-PDAC cells. Instead, we demonstrated that the impairment of pyrimidine biosynthesis was responsible for the selective response to decitabine in dep-PDAC. It has been previously recognized that oncogenic KRAS induced metabolic rewiring of nucleotide metabolism (10, 41). During the preparation of this manuscript, it was shown that the maintenance of the nucleotides pool via pyrimidine biosynthesis was indeed part of a metabolic reprogramming of KRAS dependency in PDAC and that the inhibition of KRAS-dep signaling led to a selective reduction of pyrimidine metabolites. Importantly, the inhibition of pyrimidine biosynthesis was sufficient to inhibit the growth of KRAS-dep PDAC cells (42). Along with this report, our results further support pyrimidine biosynthesis as a metabolic vulnerability for KRAS dep-PDACs tumors and demonstrate that

(*Continued.*) Colored dots represent metabolites significantly changed between control and treated conditions (adjusted *P* values <0.1). *Y*-axis shows significance level (logarithm of *P* value). *X*-axis shows $\log_2$-fold change of metabolite abundance in cells treated with decitabine relative to DMSO-treated controls; data are mean of seven biological replicates ($n = 7$). **G,** Metabolite set enrichment analysis results adapted from the MetaboAnalyst software package. Identified metabolites and their relative fold change over DMSO-treated cells were used to calculate the enrichment and statistical significance of metabolites in PA-TU-8902 cells. Top 50 perturbed pathways are shown. The dashed line indicates the cutoff of the adjusted *P* value (pV < 0.05). Color intensity (yellow to red) reflects increasing statistical significance as reported. **H,** Histogram representing selected metabolites enriched in the pyrimidine metabolism set from dep-PDAC PA-TU-8902 cells (red bars) and indep-PDAC PA-TU-8988T cells (blue bars). Histograms indicate statistically significant $\log_2$-fold change for the indicated metabolites as measured in **F**. Note that several metabolites from indep-PDAC cells are not represented because they did not have a statistically significant fold change value.

Published OnlineFirst September 5, 2019; DOI: 10.1158/0008-5472.CAN-19-0187

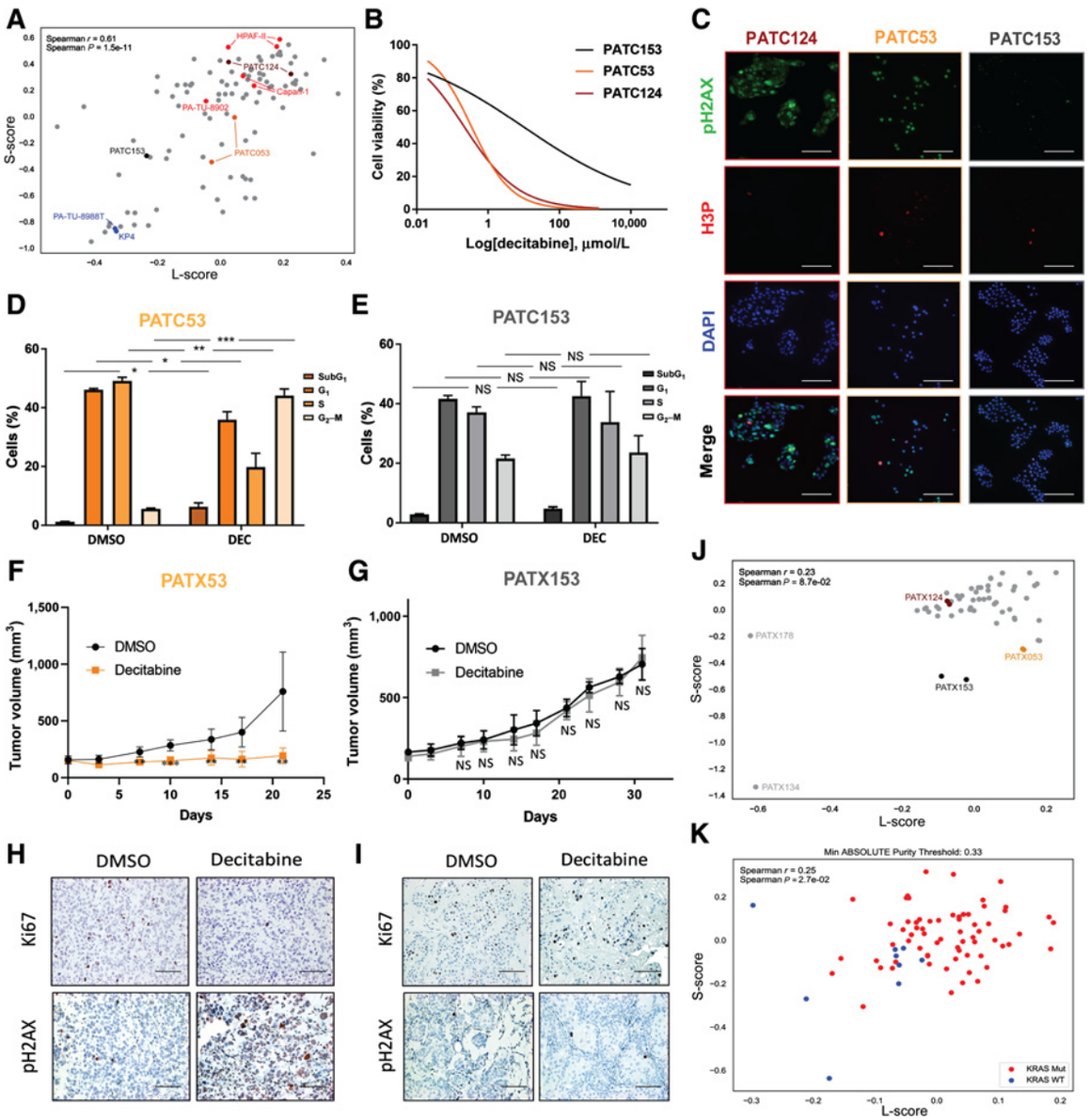

Figure 5.

Molecular signatures predict sensitivity to decitabine in selected KRAS–mutated PDX-PDAC models. **A,** Scatter plot comparing S-scores versus L-scores in a compendium of pancreatic cell lines calculated from microarray data generated from multiple sources of cell lines, including CCLE and PDX tumors ($n = 102$). Several cell lines were profiled multiple times. Blue and bright-red dots correspond to CCLE cell lines with low and high S-scores, respectively (Fig. 1A). The dark-gray, dark-red, and orange dots represent patient-derived cell lines that were tested. **B,** Cell viability of PDX-PDACs upon decitabine treatment at the indicated concentrations was assayed by ATP-based CellTiter-Glo assay. Graphs report the percentage of cell viability compared with DMSO-treated cells. **C–E,** Immunofluorescence staining (**C**) and cell-cycle analysis (**D** and **E**) in selected KRAS-dep and -indep PDX-PDACs. Cells were treated with high doses (1.25 µmol/L) of decitabine or DMSO for 3 days, and analyses were performed as described in Fig. 1. Statistical significance was calculated by two-tailed *t* test. *, $P \leq 0.05$; **, $P \leq 0.01$; ***, $P \leq 0.001$; NS, not significant. Scale bar, 100 µm. Magnification, ×20. **F** and **G,** Tumor growth kinetics of mice injected subcutaneously with one dep-PDAC (PATX53; **F**) and one indep-PDAC (PATX153; **G**) and treated i.p. with DMSO or decitabine. Tumors were collected when they reached approximately 1 cm^3 of volume. Data are mean ± SD of volumes. Differences in tumor volume were evaluated using two-tailed *t* test analysis. **, $P < 0.01$; ***, $P < 0.001$. **H** and **I,** Representative images of IHC staining of tumors from mice injected with one dep-PDAC (PATX53; **H**) and one indep-PDAC (PATX153; **I**) and collected after 1 week of treatment with DMSO or decitabine. Distinct tumor sections ($n = 3$) from three DMSO- and three decitabine-treated mice were analyzed for phospho-H2AX and Ki67 markers. Scale bar, 200 µm. Magnification, ×20. **J,** Scatter plot comparing S-scores versus L-scores in a cohort of pancreatic cancer patient–derived xenografts ($n = 49$). Dark-red and orange dots represent original PDXs of matched dep-PDAC PDX–derived cells (PATX124 and PATX53). Dark-gray dot represents a PDX model (PATX153) matched to indep-PDAC PDX–derived cell PATC153. Light-gray dots highlight two KRAS wild-type PDXs present in the cohort. **K,** Scatter plot comparing S-scores versus L-scores in the TCGA cohort of patients with pancreatic cancer (PAAD) filtered for a purity threshold of 0.33 ($n = 76$). Red and blue dots represent KRAS-mutated and wild-type cases, respectively.

decitabine is an efficacious FDA-approved drug able to target such metabolic vulnerability in KRAS-dep PDAC tumors. All together, these studies demonstrated that KRAS dependency in PDACs does induce vulnerability for drugs capable of interfering with nucleotide biosynthetic pathways. Our metabolomics studies revealed some potential mechanisms explaining how decitabine might impair pyrimidine biosynthesis and increase dUMP levels. In fact, the increase of dUMP level and its derivatives, along with a decrease of dTMP, was consistent with the inhibition of thymidylate synthase by decitabine, as previously reported (32). In addition, the induction of cytidine deaminase by decitabine (33) would also explain the reduction of dCMP. Because the increase of cellular deoxyuridine and dUMP might directly affect the rate of misincorporation of uracil into DNA, an event that leads to the increase of DNA damage, this could explain the induction of DNA damage by decitabine treatment. Moreover, we cannot rule out the additional contribution to DNA damage by the deamination of decitabine that will generate noncanonical aza-dUTPs nucleotides (33). This later will be incorporated into DNA and will be recognized as damaged bases and trigger extensive uracil glycosylase activity, resulting in DNA breaks (33, 49).

MANTRA's results for decitabine suggest a close connection between nucleotide metabolism and KRAS-dep signature, whose details began to be deciphered. Oncogenic KRAS can orchestrate the expression of metabolic genes involved with *de novo* pyrimidine biosynthesis (10). Moreover, the MYC oncogene seems to be a potential candidate, acting as a master regulator of nucleotide biosynthesis in the context of KRAS-dep pancreatic cancer (10, 42). At the same time, this model does suggest the existence of a metabolic sensor reflecting the homeostasis of nucleotide metabolism and the effects of nucleoside pyrimidine analogues. For this function, dUMP seems to be an intriguing metabolic candidate because its levels are connected with KRAS dependency, as supported by our findings as well as previous reports (10, 42). Also, dUMP level can be regulated upon treatment with decitabine by modulating nucleotide metabolism gene expression (33).

Our studies also open a new direction for PDAC patients' treatment with other nucleotide analogues, such as gemcitabine. We observed that gemcitabine, largely adopted as standard-of-care to treat patients with PDAC, was much more effective at low dosage in dep-PDACs than in indep-PDACs. In this circumstance, for selected patients whose tumor transcriptome displays a high score for genetic KRAS dependency, gemcitabine might reach a more successful efficacy-versus-toxicity ratio, with limited side effects. If this is the case, antinucleotide-based therapies would elicit increased antitumor activity in selected patients by affecting cells carrying KRAS dependency while sparing normal cells. Because clinical trials based on the treatment of patients with PDAC with gemcitabine in combination with decitabine or with decitabine in combination with inhibitors of cytidine deaminase have been conducted or are currently active, our results suggest the need to stratify patients to reach a better response rate or to retrospectively analyze patients' response rates based on KRAS dependency scores of tumors.

Our data support the potential for using molecular signature scores from tumor cells or biopsies to select better responders to decitabine, gemcitabine, and, perhaps, to MEK inhibitors as well. Poor response to MEK inhibitors in RAS-mutated cancers has been extensively reported, and it is generally linked with compensation mechanisms that lead to reactivation of ERK through upregulation of upstream pathway components such as RTKs, BRAF, or KRAS (50–52); the activation of the PI3K-AKT-mTOR pathway; or compensatory mechanisms that involve kinome reprogramming of parallel pathways (52). Moreover, clinical data failed to show trametinib to be a viable strategy to treat KRAS–mutated cancers (53–55). However, the potential for genetic KRAS independency, regardless of the KRAS mutational status, has not yet been considered as a resistance mechanism for MEK inhibitors. Notably, the L-score for KRAS dependency has been derived as a molecular response to MEK inhibitor treatment (15), and it is worth concluding that a high gene score of KRAS dependency can reflect a degree of sensitivity for the MEK inhibitor. Our *in vitro* data with trametinib treatment of PDAC cells (Fig. 3A) do support this notion, and they are in line with previous cell culture analyses showing that only a small subset of KRAS–mutant PDAC cell lines was sensitive to MEK inhibitor treatment (51, 56). Our results suggest that scoring KRAS dependency in PDAC tumors would help improve the response rate to MEK inhibitors in selected patients. However, it is also important to note that we do not expect similar cytotoxic profiles between decitabine and trametinib, because these drugs do not have a completely overlapping MoA. Although we and others have demonstrated that both drugs could downregulate pyrimidine biosynthesis in the context of KRAS dependency (56; *this article*), decitabine might have a unique propensity to generate DNA damage by accumulating dUMP or noncanonical aza-dNTPs into the DNA of cycling tumor cells, thus engaging a different cytotoxic cascade.

In conclusion, we propose a novel paradigm tailoring the clinical application of anticancer nucleoside analogues in the context of KRAS–driven rewiring of pyrimidine metabolism. Clinical trials to investigate the effectiveness of decitabine, alone or in combination, in selected KRAS-dep patients with PDAC are needed.

Disclosure of Potential Conflicts of Interest

No potential conflicts of interest were disclosed.

Authors' Contributions

Conception and design: C. Mottini, G.F. Draetta, A. Carugo, L. Cardone
Development of methodology: M. Iezzi, Y. Kang, J.B. Fleming, D. Melisi
Acquisition of data (provided animals, acquired and managed patients, provided facilities, etc.): C. Mottini, A. Lamolinara, M. Iezzi, I. Manni, J.B. Fleming, M.P. Kim, L. Cardone
Analysis and interpretation of data (e.g., statistical analysis, biostatistics, computational analysis): C. Mottini, D. Carrella, M. Iezzi, J. K. Huang, S. Buglioni, R. Minelli, C.A. Bristow, D. Trisciuoglio, A. Iuliano,. D.D. Bufalo, D.D. Bernardo, A. Carugo, L. Cardone
Writing, review, and/or revision of the manuscript: C. Mottini, H. Tomihara, D. Melisi, G.F. Draetta, G. Ciliberto, A. Carugo, L. Cardone
Administrative, technical, or material support (i.e., reporting or organizing data, constructing databases): C.A. Amoreo, F. S. Robinson, M.P. Kim
Study supervision: G. Ciliberto, L. Cardone

Acknowledgments

We thank Dr. Michele Milella (IRCCS "Regina Elena" National Cancer Institute, Rome, Italy) and Dr. Giuseppe Diaferia (IFOM, Milan, Italy) for providing PDAC cell lines. We thank Dr. Claudia Abbruzzese (IRCCS Regina Elena National Cancer Institute, Rome, Italy) and Dr. Rosanna Dattilo (ISS, Rome, Italy) for technical assistance. We thank T. Merlino ("Regina Elena" National Cancer Institute, Rome, Italy), John H. McCool (Precision Scientific Editing), and Dr. Angela K. Deem (UT MD Anderson Cancer Center) for editorial assistance and for English editing of the manuscript. We thank Dr. John Asara and the Mass Spectrometry Core Facility at the Beth Israel Deaconess Medical Center. We thank Dr. Camera E. (ISG, Rome, Italy) for assistance with metabolomics analysis. L. Cardone and C. Mottini were supported by 5 × 1000 IRE. G.F. Draetta is supported by the 2014 Pancreatic Cancer

Action Network-AACR Research Acceleration Network Grant, in memory of Skip Viragh, Grant Number 14-90-25-DRAE, and the Department of Genomic Medicine Sewell Family Chairmanship.

The costs of publication of this article were defrayed in part by the payment of page charges. This article must therefore be hereby marked *advertisement* in accordance with 18 U.S.C. Section 1734 solely to indicate this fact.

Received January 17, 2019; revised July 24, 2019; accepted August 29, 2019; published first September 5, 2019.

References

1. Siegel RL, Miller KD, Jemal A. Cancer statistics, 2017. CA Cancer J Clin 2017;67:7–30.
2. Kleeff J, Korc M, Apte M, La Vecchia C, Johnson CD, Biankin AV, et al. Pancreatic cancer. Nat Rev Dis Primers 2016;2:16022.
3. Kanda M, Matthaei H, Wu J, Hong SM, Yu J, Borges M, et al. Presence of somatic mutations in most early-stage pancreatic intraepithelial neoplasia. Gastroenterology 2012;142:730–3.
4. Hingorani SR, Petricoin EF, Maitra A, Rajapakse V, King C, Jacobetz MA, et al. Preinvasive and invasive ductal pancreatic cancer and its early detection in the mouse. Cancer Cell 2003;4:437–50.
5. Jones S, Zhang X, Parsons DW, Lin JC, Leary RJ, Angenendt P, et al. Core signaling pathways in human pancreatic cancers revealed by global genomic analyses. Science 2008;321:1801–6.
6. Simanshu DK, Nissley DV, McCormick F. RAS proteins and their regulators in human disease. Cell 2017;170:17–33.
7. Nussinov R, Tsai CJ, Chakrabarti M, Jang H. A new view of Ras isoforms in cancers. Cancer Res 2016;76:18–23.
8. Castellano E, Santos E. Functional specificity of ras isoforms: so similar but so different. Genes Cancer 2011;2:216–31.
9. Collins MA, Bednar F, Zhang Y, Brisset JC, Galban S, Galban CJ, et al. Oncogenic Kras is required for both the initiation and maintenance of pancreatic cancer in mice. J Clin Invest 2012;122:639–53.
10. Ying H, Kimmelman AC, Lyssiotis CA, Hua S, Chu GC, Fletcher-Sananikone E, et al. Oncogenic Kras maintains pancreatic tumors through regulation of anabolic glucose metabolism. Cell 2012;149:656–70.
11. Bild AH, Yao G, Chang JT, Wang Q, Potti A, Chasse D, et al. Oncogenic pathway signatures in human cancers as a guide to targeted therapies. Nature 2006;439:353–7.
12. Furge KA, Tan MH, Dykema K, Kort E, Stadler W, Yao X, et al. Identification of deregulated oncogenic pathways in renal cell carcinoma: an integrated oncogenomic approach based on gene expression profiling. Oncogene 2007;26:1346–50.
13. Nevins JR, Potti A. Mining gene expression profiles: expression signatures as cancer phenotypes. Nat Rev Genet 2007;8:601–9.
14. Qian J, Niu J, Li M, Chiao PJ, Tsao MS. In vitro modeling of human pancreatic duct epithelial cell transformation defines gene expression changes induced by K-ras oncogenic activation in pancreatic carcinogenesis. Cancer Res 2005;65:5045–53.
15. Loboda A, Nebozhyn M, Klinghoffer R, Frazier J, Chastain M, Arthur W, et al. A gene expression signature of RAS pathway dependence predicts response to PI3K and RAS pathway inhibitors and expands the population of RAS pathway activated tumors. BMC Med Genomics 2010;3:26.
16. Tsang YH, Dogruluk T, Tedeschi PM, Wardwell-Ozgo J, Lu H, Espitia M, et al. Functional annotation of rare gene aberration drivers of pancreatic cancer. Nat Commun 2016;7:10500.
17. Singh A, Greninger P, Rhodes D, Koopman L, Violette S, Bardeesy N, et al. A gene expression signature associated with "K-Ras addiction" reveals regulators of EMT and tumor cell survival. Cancer Cell 2009;15:489–500.
18. Janes MR, Zhang J, Li LS, Hansen R, Peters U, Guo X, et al. Targeting KRAS mutant cancers with a covalent G12C-specific inhibitor. Cell 2018;172:578–89.
19. Bailey P, Chang DK, Nones K, Johns AL, Patch AM, Gingras MC, et al. Genomic analyses identify molecular subtypes of pancreatic cancer. Nature 2016;531:47–52.
20. Dang CV, Reddy EP, Shokat KM, Soucek L. Drugging the "undruggable" cancer targets. Nat Rev Cancer 2017;17:502–8.
21. Carrella D, Manni I, Tumaini B, Dattilo R, Papaccio F, Mutarelli M, et al. Computational drugs repositioning identifies inhibitors of oncogenic PI3K/AKT/P70S6K-dependent pathways among FDA-approved compounds. Oncotarget 2016;7:58743–58.
22. Carrella D, Napolitano F, Rispoli R, Miglietta M, Carissimo A, Cutillo L, et al. Mantra 2.0: an online collaborative resource for drug mode of action and repurposing by network analysis. Bioinformatics 2014;30:1787–8.
23. Cardone L. Biocomputing drug repurposing toward targeted therapies. Aging (Albany NY) 2016;8:2609–10.
24. Ganguly S, Amin M, Divine C, Aljitawi OS, Abhyankar S, McGuirk JP. Decitabine in patients with relapsed acute myeloid leukemia (AML) after allogeneic stem cell transplantation (allo-SCT). Ann Hematol 2013;92:549–50.
25. Kantarjian HM. Recent experience with decitabine in MDS. Clin Adv Hematol Oncol 2007;5:140.
26. Stresemann C, Lyko F. Modes of action of the DNA methyltransferase inhibitors azacytidine and decitabine. Int J Cancer 2008;123:8–13.
27. Estey EH. Epigenetics in clinical practice: the examples of azacitidine and decitabine in myelodysplasia and acute myeloid leukemia. Leukemia 2013;27:1803–12.
28. Mini E, Nobili S, Caciagli B, Landini I, Mazzei T. Cellular pharmacology of gemcitabine. Ann Oncol 2006;17Suppl 5:v7–12.
29. Cerqueira NM, Fernandes PA, Ramos MJ. Understanding ribonucleotide reductase inactivation by gemcitabine. Chemistry 2007;13:8507–15.
30. Schelhaas S, Held A, Wachsmuth L, Hermann S, Honess DJ, Heinzmann K, et al. Gemcitabine mechanism of action confounds early assessment of treatment response by 3′-deoxy-3′-[18F]fluorothymidine in preclinical models of lung cancer. Cancer Res 2016;76:7096–105.
31. Honeywell RJ, Ruiz van Haperen VW, Veerman G, Smid K, Peters GJ. Inhibition of thymidylate synthase by 2′,2′-difluoro-2′-deoxycytidine (Gemcitabine) and its metabolite 2′,2′-difluoro-2′-deoxyuridine. Int J Biochem Cell Biol 2015;60:73–81.
32. Almqvist H, Axelsson H, Jafari R, Dan C, Mateus A, Haraldsson M, et al. CETSA screening identifies known and novel thymidylate synthase inhibitors and slow intracellular activation of 5-fluorouracil. Nat Commun 2016;7:11040.
33. Requena CE, Perez-Moreno G, Horvath A, Vertessy BG, Ruiz-Perez LM, Gonzalez-Pacanowska D, et al. The nucleotidohydrolases DCTPP1 and dUTPase are involved in the cellular response to decitabine. Biochem J 2016;473:2635–43.
34. Kim MP, Evans DB, Wang H, Abbruzzese JL, Fleming JB, Gallick GE. Generation of orthotopic and heterotopic human pancreatic cancer xenografts in immunodeficient mice. Nat Protoc 2009;4:1670–80.
35. Carugo A, Genovese G, Seth S, Nezi L, Rose JL, Bossi D, et al. In vivo functional platform targeting patient-derived xenografts identifies WDR5-Myc association as a critical determinant of pancreatic cancer. Cell Rep 2016;16:133–47.
36. Lee KE, Bar-Sagi D. Oncogenic KRas suppresses inflammation-associated senescence of pancreatic ductal cells. Cancer Cell 2010;18:448–58.
37. Grasso D, Bintz J, Lomberk G, Molejon MI, Loncle C, Garcia MN, et al. Pivotal role of the chromatin protein Nupr1 in Kras-induced senescence and transformation. Sci Rep 2015;5:17549.
38. Barretina J, Caponigro G, Stransky N, Venkatesan K, Margolin AA, Kim S, et al. The Cancer Cell Line Encyclopedia enables predictive modelling of anticancer drug sensitivity. Nature 2012;483:603–7.
39. Chou TC. Theoretical basis, experimental design, and computerized simulation of synergism and antagonism in drug combination studies. Pharmacol Rev 2006;58:621–81.
40. Chou TC. Drug combination studies and their synergy quantification using the Chou-Talalay method. Cancer Res 2010;70:440–6.
41. Koundinya M, Sudhalter J, Courjaud A, Lionne B, Touyer G, Bonnet L, et al. Dependence on the pyrimidine biosynthetic enzyme DHODH is a synthetic lethal vulnerability in mutant KRAS-driven cancers. Cell Chem Biol 2018;25:705–17.

42. Santana-Codina N, Roeth AA, Zhang Y, Yang A, Mashadova O, Asara JM, et al. Oncogenic KRAS supports pancreatic cancer through regulation of nucleotide synthesis. Nat Commun 2018;9:4945.
43. Knudsen ES, Balaji U, Mannakee B, Vail P, Eslinger C, Moxom C, et al. Pancreatic cancer cell lines as patient-derived avatars: genetic characterisation and functional utility. Gut 2018;67:508–20.
44. Siolas D, Hannon GJ. Patient-derived tumor xenografts: transforming clinical samples into mouse models. Cancer Res 2013;73:5315–9.
45. Tentler JJ, Tan AC, Weekes CD, Jimeno A, Leong S, Pitts TM, et al. Patient-derived tumour xenografts as models for oncology drug development. Nat Rev Clin Oncol 2012;9:338–50.
46. Luo J, Emanuele MJ, Li D, Creighton CJ, Schlabach MR, Westbrook TF, et al. A genome-wide RNAi screen identifies multiple synthetic lethal interactions with the Ras oncogene. Cell 2009;137:835–48.
47. Singh A, Sweeney MF, Yu M, Burger A, Greninger P, Benes C, et al. TAK1 inhibition promotes apoptosis in KRAS-dependent colon cancers. Cell 2012;148:639–50.
48. Boutin AT, Liao WT, Wang M, Hwang SS, Karpinets TV, Cheung H, et al. Oncogenic Kras drives invasion and maintains metastases in colorectal cancer. Genes Dev 2017;31:370–82.
49. Boorstein RJ, Chiu LN, Teebor GW. A mammalian cell line deficient in activity of the DNA repair enzyme 5-hydroxymethyluracil-DNA glycosylase is resistant to the toxic effects of the thymidine analog 5-hydroxymethyl-2′-deoxyuridine. Mol Cell Biol 1992;12:5536–40.
50. Little AS, Balmanno K, Sale MJ, Newman S, Dry JR, Hampson M, et al. A correction to the research article titled: "Amplification of the driving oncogene, KRAS or BRAF, underpins acquired resistance to MEK1/2 inhibitors in colorectal cancer cells" by A. S. Little, K. Balmanno, M. J. Sale, S. Newman, J. R. Dry, M. Hampson, P. A. W. Edwards, P. D. Smith, S. J. Cook. Sci Signal 2011;4:er2.
51. Hayes TK, Neel NF, Hu C, Gautam P, Chenard M, Long B, et al. Long-term ERK inhibition in KRAS-mutant pancreatic cancer is associated with MYC degradation and senescence-like growth suppression. Cancer Cell 2016;29:75–89.
52. Ryan MB, Der CJ, Wang-Gillam A, Cox AD. Targeting RAS-mutant cancers: is ERK the key? Trends Cancer 2015;1:183–98.
53. Infante JR, Somer BG, Park JO, Li CP, Scheulen ME, Kasubhai SM, et al. A randomised, double-blind, placebo-controlled trial of trametinib, an oral MEK inhibitor, in combination with gemcitabine for patients with untreated metastatic adenocarcinoma of the pancreas. Eur J Cancer 2014;50:2072–81.
54. Kasuga A, Nakagawa K, Nagashima F, Shimizu T, Naruge D, Nishina S, et al. A phase I/Ib study of trametinib (GSK1120212) alone and in combination with gemcitabine in Japanese patients with advanced solid tumors. Invest New Drugs 2015;33:1058–67.
55. Tolcher AW, Bendell JC, Papadopoulos KP, Burris HA 3rd, Patnaik A, Jones SF, et al. A phase IB trial of the oral MEK inhibitor trametinib (GSK1120212) in combination with everolimus in patients with advanced solid tumors. Ann Oncol 2015;26:58–64.
56. Witkiewicz AK, McMillan EA, Balaji U, Baek G, Lin WC, Mansour J, et al. Whole-exome sequencing of pancreatic cancer defines genetic diversity and therapeutic targets. Nat Commun 2015;6:6744.

Published OnlineFirst September 5, 2019; DOI: 10.1158/0008-5472.CAN-19-0187

Cancer Research
The Journal of Cancer Research (1916–1930) | The American Journal of Cancer (1931–1940)

AACR American Association for Cancer Research

Predictive Signatures Inform the Effective Repurposing of Decitabine to Treat KRAS–Dependent Pancreatic Ductal Adenocarcinoma

Carla Mottini, Hideo Tomihara, Diego Carrella, et al.

Cancer Res 2019;79:5612-5625. Published OnlineFirst September 5, 2019.